Placenta 30 (2009) 88–95

Contents lists available at ScienceDirect

Placenta

journal homepage: www.elsevier.com/locate/placenta

Murine Abortion is Associated with Enhanced Hyaluronan Expression and Abnormal Localization at the Fetomaternal Interface

R. Cordo-Russo [a,b], M.G. Garcia [a,b], G. Barrientos [a], A.S. Orsal [a], M. Viola [c], P. Moschansky [a], F. Ringel [a], A. Passi [c], L. Alaniz [d], S. Hajos [b], S.M. Blois [a,*]

[a] University Medicine Berlin, Charité Centrum 12 Internal Medicine and Dermatology, Biomedical Research Building, Campus Virchow, Augustenburger Platz 1, 13353 Berlin, Germany
[b] Cátedra de Inmunología-IDEHU, Facultad de Farmacia y Bioquímica, Universidad de Buenos Aires, UBA-CONICET, 1113 Buenos Aires, Argentina
[c] Dipartimento di Scienze Biomediche Sperimentali e Cliniche, Università degli Studi dell'Insubria, Via Dunant 5, 21100 Varese, Italy
[d] Laboratorio de Terapia Génica, Facultad de Ciencias Biomédicas, Universidad Austral, 1635 Pilar, Buenos Aires, Argentina

ARTICLE INFO

Article history:
Accepted 26 October 2008

Keywords:
Hyaluronan
Hyaluronan molecular size
Hyaluronan synthases
Hyaluronidases
Murine pregnancy

ABSTRACT

The remodelling of the endometrial architecture is fundamental to create a suitable environment for the establishment of pregnancy. During this process, substantial alterations in the composition of maternal extracellular matrix play an important role by providing a prosperous medium for implantation as well as modulating trophoblast invasion leading to the formation of a functional placental unit.
Hyaluronan is a conspicuous component of the extracellular matrix, particularly in remodelling tissues undergoing regeneration and repair. During gestation, changes in HA deposition and distribution indicate that this molecule may participate in preparation of the endometrial stroma for reception and implantation of the embryo. However, little is known about the role of hyaluronan at the fetomaternal interface, specially regarding its influence in pregnancy outcome.
In the present study we show increased decidual hyaluronan levels in spontaneous abortion compared with normal pregnancy mice on gestation day 7.5. Both in normal and pathologic pregnancies, high molecular size hyaluronan was found at the fetomaternal unit. However, hyaluronan metabolism (which results from the activity of hyaluronan synthases and hyaluronidases) seems to be altered in spontaneous abortion as shown by a decrease in Hyal-3 expression as well as by differences in hyaluronan molecular size spectrum. This alteration in hyaluronan metabolism in spontaneous abortion could explain its increased concentration observed in decidua and the abnormal distribution of hyaluronan around the embryo implantation crypt. Thus, increased decidual hyaluronan levels resulting from abnormal deposition and turn over may contribute to the pathogenesis of pregnancy failure.

1. Introduction

Successful implantation and pregnancy establishment are unique biological events characterized by delicate interactions between the conceptus and the maternal environment. Development of the embryo to the blastocyst stage, its adhesion to the endometrium and subsequent invasion of the underlying stroma leading to formation of a functional placenta are the result of complex regulatory mechanisms that involve endometrial modifications as well as maternal immunological tolerance [1]. Despite being critical to the survival of the species, mammalian reproduction is relatively inefficient. Indeed, the highest probability of conception during a menstrual cycle is as low as 30 percent. Furthermore, in humans, approximately 25 percent of all conceptions last beyond 20 weeks of gestation. Although many studies have been developed, the mechanisms that determine pregnancy maintenance are still largely elusive.

In rodents, pregnancy lasts between 19 and 20 days. Implantation of the blastocyst involves adhesion and invasion of endometrium and takes place between gestation days (Gd) 4–5. During pregnancy establishment, the endometrium is transformed into a highly specialized decidual tissue; a process referred to as decidualization that not only implicates proliferation of endometrial stromal cells into decidual cells but also formation of new vasculature [2]. Afterwards, the placentation process takes place. The placenta plays a crucial role since it constitutes the contact surface between mother and fetus (the fetomaternal interface) and allows the physiological exchange of gases, nutrients and waste products. Mice, as well as humans, present a haemochorial placentation characterized by trophoblast cells eroding the

* Corresponding author. Tel.: +49 30 450 553863; fax: +49 30 450 553997.
E-mail address: sandra.blois@charite.de (S.M. Blois).

0143-4004/$ – see front matter © 2008 Elsevier Ltd. All rights reserved.
doi:10.1016/j.placenta.2008.10.013

maternal vasculature resulting in direct contact between maternal blood and embryonic trophoblast cells. In spite of the differences between mice and human placentation [3], mice still constitute a useful model to understand the gestation process.

The remodelling of the endometrial architecture is fundamental to create a suitable environment for blastocyst implantation. This process includes phases of cellular proliferation, differentiation and tissue breakdown along with alterations in the composition of maternal extracellular matrix (ECM) [4]. The ECM remodelling plays an important role providing a prosperous medium for implantation and modulating trophoblast invasion leading to the establishment of a functional placental unit [5].

Hyaluronan (HA) is a conspicuous component of the ECM especially in remodelling tissues [6]. HA is a linear glycosaminoglycan (GAG), composed of repeated disaccharide units of glucuronic acid and N-acetylglucosamine, that exists as a high molecular weight polymer ranging from 10^5 to 10^7 Da. HA differs from other GAGs specially in its synthesis and degradation. HA biosynthesis is carried out at the inner face of the plasma membrane by hyaluronan synthases (HAS) and the growing polymer is extruded through the membrane into the extracellular space. In mammals, there are three HAS isozymes: HAS-1, HAS-2 and HAS-3 [7]. Though the synthases can be regulated, the major control for HA deposition occurs at catabolism. Degradation of HA occurs by the concerted action of three enzymes: a hyaluronidase (Hyal) and two exoglycosidases. In humans, six hyaluronidase genes have been identified. These are *HYAL-1*, *HYAL-2*, *HYAL-3*, *HYAL-4*, *SPAM1* and *PHYAL-1*, which, respectively, encode HYAL-1, HYAL-2, HYAL-3, HYAL-4, PH-20 and a pseudogene transcribed but not translated [8]. Mouse genome presents a seventh hyaluronidase-like gene called *Hyal-5*. Among the Hyals, HYAL-1 and HYAL-2 are of great importance in degradation of high molecular weight HA (HMW-HA > 1000 kDa). Differential expression of the enzymes related with HA synthesis and degradation has been observed in tumors and during development [6,9]. However, their role remains to be completely clarified.

Despite its simple chemical composition, HA possesses several functions both in physiological and pathological conditions such as morphogenesis, tissue injury and repair, inflammation, and tumorigenesis [6,10–12]. HA is prominent during embryonic development and at sites of wound healing. In healthy tissues, HA regulates water homeostasis, influencing hydration and physical properties of tissues. Interaction of HA with other ECM components (proteoglycan, aggrecan, or versican) allows the assembly of many tissues. Moreover, upon interaction with CD44, RHAMM (receptor for hyaluronic acid mediated motility), TLR-4 (Toll like receptor 4) cell surface receptors or different HA binding-proteins (TSG-6, SHAP), HA is able to modulate fundamental cell behaviours such as adhesion, migration, proliferation and differentiation [13]. The molecular weight and concentration of HA are also important in determining their functions. For example, HMW-HA has been shown to be anti-angiogenic, while HA fragments (3–25 disaccharide units) induced angiogenesis *in vitro* [14]. Besides, HA fragments have been found to be potent activators of dendritic cells and to induce proinflammatory cytokine secretion that could not be exerted by HMW-HA [15]. As nearly all of the studies have been performed *in vitro*, the challenge is to characterize *in vivo* the size of HA in the local microenvironment and to clarify its role.

During gestation, changes in HA deposition and distribution indicate that HA may participate in preparation of the endometrial stroma for reception and implantation of the embryo [16–19]. Little is known however about the role of HA at the fetomaternal interface, especially regarding its influence in pregnancy outcome. Consequently, the aim of this work was to analyze the levels, distribution, synthesis and degradation, and molecular size of HA during murine normal and pathologic pregnancies. The present study was performed using a normal pregnancy mouse model, BALB/c-mated CBA/J females, and an abortion prone mating, DBA/2J-mated CBA/J females. Findings in the latter model are of great importance to further understand the role of HA during normal pregnancy and spontaneous abortion.

2. Materials and methods

2.1. Animals

Mice were purchased from Charles River and maintained in an animal facility with a 12 h light/dark cycle. All animal experiments were conducted according to institutional guidelines of the Medicine University of Berlin. CBA/J females were caged with DBA/2J or BALB/c males overnight and examined for a vaginal plug the next morning. The presence of the plug determined the day 0.5 of pregnancy. After that the pregnant females were segregated. The CBA/J females mated both with BALB/c (normal pregnancy) or DBA/2J (spontaneous abortion) were sacrificed on gestation days (Gd) 7.5 ($n = 6$ per group) and 13.5 ($n = 6$ per group). After the mice were killed, the abdomen was carefully opened and access to the uterus was gained by pushing intestinal tissue to the side. The uterus was then removed by surgical cuts at the cervix and the ovaries. Decidua and placenta were removed and divided into pieces. Particularly, on Gd 7.5 decidua at the site of implantation was carefully peeled from the embryo and former placenta which were discarded. Afterwards, tissue extracts were immediately prepared from one section while other sections were frozen for RT-PCR and analysis of HA molecular size. For histochemistry, the complete fetal and maternal unit at the site of implantation was frozen. Before sacrifice, blood samples were obtained by retro-orbital bleeding under anaesthesia for HA level measurement. Non-pregnant mice were used as controls and both blood and uteri were processed as explained below. Determination of estrous cycle stages was performed as previously described [20].

2.2. Tissue extracts and serum collection

Tissue extracts were prepared using a Total Protein Extraction Kit (# 2140, Chemicon International) as described by the manufacturer. Briefly, tissue were suspended in ice-cold homogenization buffer, homogenized and incubated for 20 min at 4 °C. Then, tissue extracts were clarified by centrifugation at 11.000 rpm for 20 min and stored at −80 °C [21]. Blood withdrawn by retro-orbital bleeding was centrifuged at 6000 rpm for 20 min at 4 °C, and the decanted serum was stored at −80 °C.

2.3. Measurement of HA levels by enzyme linked immunosorbent assay (ELISA)

HA levels in serum and tissue extracts from decidua and placenta were measured with a competitive ELISA as described before [22]. We studied HA levels on Gd 7.5 since this a critical time period for sustaining fetal survival in mice, whereas Gd 13.5 was examined as an advanced time point in pregnancy in which resorption (abortion sites) are visible. As a control, HA measurement in uterus extracts from non-pregnant mice was also performed. In this assay, HA of different molecular sizes, HMW- and fragmented HA, are determined. Ninety-six well microtiter plates (Nunc) were coated with 25 μg/ml HMW-HA (CPN spol. s.r.o Czech Republic, Farmatrade Argentina). The HA-coated wells were incubated with 50 μl of sample (diluted 1/20) or standard HMW-HA (ranging from 0 to 2 μg/ml), in the presence of 0.5 μg/ml biotinylated HA binding protein (bHABP) (# 385911, Calbiochem). After incubation at 37 °C for 4 h, washes in PBS containing 0.05% Tween 20 were performed. The bHABP bound to the wells was determined using an avidin–biotin detection system (# A2004, Vector). Sample concentrations were calculated from a standard curve generated by plotting the absorbance at 490 nm against the concentration of HMW-HA.

2.4. HA staining

The staining was performed as described before [23]. Briefly, cryostat sections (10 μm) were incubated with 3% H_2O_2 in methanol for 30 min at RT to block endogenous peroxidase, followed by avidin, biotin and protein blocking solution (Vector). Then, 5 μg/ml bHABP (# 385911, Calbiochem) diluted in PBS containing 1% BSA was applied for 1 h. Control sections were stained with bHABP that had been pretreated with 100 U/ml Streptomyces hyaluronidase (# H3506, Sigma) in PBS at 37 °C for 30 min. As amplification and revealing system, we used peroxidase complex (Vector) 1:100 in PBS for 30 min. The signal was detected by incubating sections with 0.2 mg/ml diaminobenzidine (DAB) (Sigma) and 0.05% H_2O_2, followed by light counterstaining with 0.1% Mayer's hematoxylin. Slides were examined using a Zeiss Axioscope light microscope (Jena). Photodocumentation was performed using digital image analysis system (Zeiss KS400, Jena).

2.5. Total RNA extraction and semiquantitative reverse transcription polymerase chain reaction (RT-PCR)

Decidua or placenta tissues (100 mg) were treated with 1 ml TRIzol (# 15596-026, Invitrogen) and disaggregated using a homogenizer. Total RNA was extracted

according to the manufacturer's instructions. Isolated RNA was dissolved in water and analyzed by spectrophotometry to determine RNA concentration, yield and purity (OD260/OD280 1.7–2. Reverse transcription was performed from 1 μg total RNA using 100 ng of random primer (# 48190-011, Invitrogen) in a 20 μl reaction volume containing 200 U Superscript II (# 18064-014, Invitrogen), 0.01 M dithiothreitol (DTT), 10 mM dNTPs and 40 U RNaseOUT (# 1077-019, Invitrogen). The mixture was incubated at 42 °C for 50 min and then at 70 °C for 15 min. cDNA was then amplified with specific primers for *HAS-1*, *HAS-2*, *HAS-3*, *Hyal-1*, *Hyal-2* and *Hyal-3* as previously described by Mummert et al. [24], see Table 1. Thirty-five PCR cycles were carried out with an annealing temperature of 53 °C (for *Hyal-3*), 60 °C (for *Hyal-1*) and 57 °C (for the others), followed by a 10 min extension at 72 °C. To ensure that load was kept constant in all lanes, *hprt* gene was amplified by 30 cycles (60 s at 94 °C, 60 s at 60 °C and 60 s at 72 °C) followed by 10 min extension at 72 °C. PCR products were separated by agarose gel electrophoresis (2%) and stained with ethidium bromide. Photodocumentation was performed using the UV transilluminator Eagle Eye II (Stratagene).

2.6. Measurement of hyaluronidase activities (ELISA like assay)

Hyaluronidase (Hyal) activity present in decidua and placenta extracts was measured using an ELISA like assay as described before [22,25]. Briefly, the wells in a 96 well microtiter plate were coated with 200 μg/ml HMW-HA. The HA-coated plates were incubated with 50 μl of sample (decidua diluted 1/5, placenta diluted 1/10) or standard bovine testis hyaluronidase (# 385931, Calbiochem) for 16 h at 37 °C in Hyal assay buffer (0.1 M sodium formate, 0.15 M NaCl, 0.2 mg/ml bovine serum albumin). Following incubation, remaining HA was determined using 5 μg/ml bHABP and an avidin–biotin detection system as in the HA-ELISA assay. To calculate Hyal activity, a standard curve was prepared by plotting the absorbance at 490 nm versus Hyal activity from standard Hyal (milliunits/ml). All activity determinations were normalized to protein concentration (milliunits/mg). The pH activity profile of placenta and decidua derived Hyal were determined by incubating HA-coated wells with tissue extracts in Hyal assay buffer at various pH values (1.5–6.5). Between pH 3.0 and 4.5, Hyal activity was tested in buffers differing by 0.1 pH unit, while at other pH the buffers differed by 0.5 pH unit. As control, wells were incubated with buffers of specified pH. The results were expressed as (Absorbance control − Absorbance sample) × 100. The maximum difference was designated as 100% and data was expressed as a percentage of maximum.

2.7. Analysis of HA molecular size

For analysis of HA molecular size, GAGs were first isolated as described elsewhere [26]. Briefly, frozen samples of decidua and placenta (50 mg each) were suspended in 300 μl of 0.1 M ammonium acetate pH 7.0, and digested with protease K (# P6556, Sigma) at 60 °C for 2 h. After enzyme inactivation, 1.2 ml ethanol 96% was added and the mixture was frozen at −20 °C overnight to precipitate the GAGs. After centrifugation at 10,000 × g at 4 °C for 15 min, the pellets were solubilised with 100 μl of 0.1 M ammonium acetate pH 7.0 by gently mixing with a pipette. GAGs were derivatized as described by Calabro et al. [27] to increase the absorbance signal at 280 nm.

Separation of GAGs was performed using Fast Protein Liquid Chromatography (FPLC) (AKTA Amersham Pharmacia Biotech). Gel chromatography was carried out using a Superdex™ 200 HR 10/30 prepacked column (10 mm internal diameter, 30–31 cm height of the packed bed, Amersham Pharmacia Biotech) at room temperature. The buffer used was 0.1 M ammonium acetate, pH 7.0, with 0.05% Tween 20, and the flow rate was 0.35 ml/min. Sample peaks elution was monitored following the absorbance at 280 nm. The identification of polysaccharides was performed using FACE on each fraction collected (2 ml each). Briefly, the fractions were digested with 100 mU/ml Hyaluronidase SD at 37 °C for 1 h and 100 mU/ml Chondroitinase ABC at 37 °C for 3 h. The obtained unsaturated disaccharides were derivatized with AMAC and analyzed by FACE [27,28].

Table 1
Primer sequences for mouse *HAS-1*, *HAS-2*, *HAS-3*, *Hyal-1*, *Hyal-2*, *Hyal-3* and *hprt*.

	Primer sequence	Product size (bp)
HAS-1		
Sense	5′-GGAAAGCTTGACTCAGACACAAGAC-3′	553
Antisense	5′-AGGGAATTCGTATAGCCACTCTCGG-3′	
HAS-2		
Sense	5′-TGGAACACCGGAAAATGAAGAAG-3′	805
Antisense	5′-GGACCGAGCCGTGTATTTAGTTGC-3′	
HAS-3		
Sense	5′-CCATGAGGCGGGTGAAGGAGAG-3′	752
Antisense	5′-ATGCGGCCACGGTAGAAAAGTTGT-3′	
Hyal-1		
Sense	5′-TATCCAACCGGCCATTCATCACTG-3′	992
Antisense	5′-ATACCCCCGCTTGTCACACCACTTG-3′	
Hyal-2		
Sense	5′-CATCTTCACTGGCCGACCCTTTGT-3′	1220
Antisense	5′-TCGCCACCCCAGCCCAGATAGC-3′	
Hyal-3		
Sense	5′-CCTAGGCCTAATGATGGTG-3′	507
Antisense	5′-GCTAGTATGGGCTTTGTGG-3′	
hprt		
Sense	5′-GTT GGA TAC AGG CCA GAC TTT GT 3′	225
Antisense	5′-CAC AGG ACT AGA ACA CCT GC 3′	

2.8. Statistical analysis

All the experiments were carried out at least in triplicate. Statistical significance of evaluated data was tested using one-way ANOVA and Tukey's test. p values < 0.05 or less were regarded as statistically significant. Analysis was performed using Prism software (Graph Pad).

3. Results

3.1. Changes of HA peripheral and local levels during pregnancy

Considering that modification in ECM components, particularly in HA deposition, takes place during pregnancy [17,19], we first evaluated HA levels in normal pregnancy (BALB/c-mated CBA/J females) and spontaneous abortion (DBA/2J-mated CBA/J females) models. An ELISA assay was used to determine HA concentration in serum and decidua extracts on Gd 7.5 and 13.5 as well as in placenta extracts on Gd 13.5.

Serum HA levels in non-pregnant mice (∼2 μg/ml) were similar to those observed in normal pregnancy and spontaneous abortion on Gd 7.5. Moreover, we observed a significant increase in HA serum concentration during normal pregnancy, when comparing Gd 7.5 and 13.5 ($p < 0.01$). However, spontaneous abortion mice showed uniform HA serum levels throughout gestation (Fig. 1A). In Gd 13.5, serum HA levels were significantly lower in the spontaneous abortion model compared with the normal pregnancy group ($p < 0.05$).

The decidual HA levels were increased in normal pregnancy on Gd 13.5 compared to Gd 7.5 ($p < 0.001$), indicating that changes in HA levels occur along with the normal process of decidualization. However, we were not able to find significant changes in HA concentration at decidua from spontaneous abortion mice throughout gestation. Interestingly, on Gd 7.5 decidual HA levels from spontaneous abortion showed a significant increase when compared with normal pregnancy mice ($p < 0.01$) (Fig. 1B). It is noteworthy that HA levels in decidua from spontaneous abortion were 7 and 4 fold higher than in serum both on Gd 7.5 and 13.5 respectively. In normal pregnancy, although there was an increase in HA concentration throughout gestation, no significant differences were observed when comparing decidual and serum HA levels both on Gd 7.5 and 13.5.

In placenta, no differences between normal pregnancy and spontaneous abortion were observed. However, placental HA levels were 10 and 8 fold lower as compared with decidual levels in normal pregnancy and spontaneous abortion respectively (Fig. 1C).

Taken together, these data showed that in normal pregnancy HA increases throughout gestation observing a correlation between changes in serum and in decidual levels. However, such correlation was not evident in spontaneous abortion mice, which showed clearly increased decidual HA in comparison to serum HA.

3.2. Localization of HA during pregnancy

Differential HA levels were observed between normal pregnancy and spontaneous abortion. Thus, our next aim was to analyze HA tissue distribution at the fetomaternal interface by histochemistry.

First, we evaluated HA presence in different phases of the estrous cycle in non-pregnant mice. The estrous cycle is 98–106 h long and is divided in four stages: proestrus, estrus (which

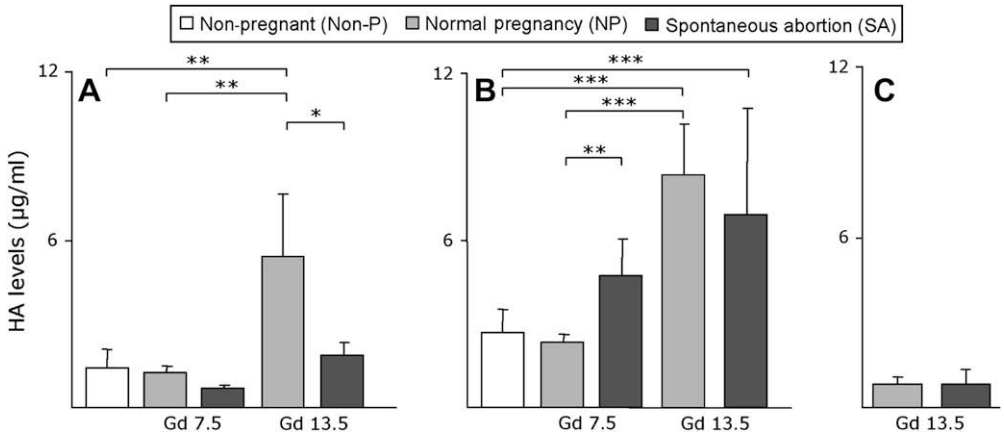

Fig. 1. Changes in HA levels during pregnancy. Measurement of HA levels in serum (A), decidua (B) and placenta (C) from non-pregnant, normal pregnancy and spontaneous abortion mice by ELISA as described in "Section 2". In pregnant mice, serum and decidual HA levels were evaluated on Gd 7.5 and 13.5, while placental HA was studied on Gd 13.5. Data in the diagram is depicted as the mean ± SEM ($n = 6$). $^{***}p < 0.001$, $^{**}p < 0.01$ and $^{*}p < 0.05$.

culminates with ovulation), metestrus and diestrus. Thus, we decided to study HA expression in the stages surrounding ovulation in mice. Histochemistry for HA was performed in uterus from estrus and metestrus period and in both cases HA was found in the myometrium as well as in endometrial tissue (Fig. 2A and B), its staining intensity being particularly stronger in endometrium stroma (Fig. 2C–F). However, HA expression could not be detected in the endometrium lumen or glands.

On day 7.5 of both normal and pathological pregnancies, HA was localized in the myometrium and mesometrial decidua (Fig. 2G and H). However, only spontaneous abortion mouse tissue expressed HA around the embryo implantation crypt (Fig. 2). This finding is in accordance with the increased decidual levels of HA observed in spontaneous abortion mice on Gd 7.5. We also evaluated HA expression in placenta on Gd 13.5. As shown in Fig. 2K and L, no HA signal could be detected in either of the mating combinations analyzed. However, a signal appeared surrounding umbilical blood vessels (Fig. 2K and L inserts).

3.3. HA synthesis and degradation during pregnancy

To identify the enzymes involved in HA synthesis and degradation, we evaluated mRNA expression for HAS (*HAS-1*, *HAS-2* and *HAS-3*) and Hyal (*Hyal-1*, *Hyal-2* and *Hyal-3*) by RT-PCR in decidual and placental tissue extracts.

On Gd 7.5, *HAS-1* and *HAS-2* mRNA were increased in normal pregnancy compared to spontaneous abortion decidua ($p < 0.05$), while no changes were observed in *HAS-3*, *Hyal-1* and *Hyal-2* mRNA. Interestingly, expression levels of *Hyal-3* mRNA were 2 fold increased in decidua from normal pregnancy mice compared to spontaneous abortion ($p < 0.01$) (Fig. 3A and B). In addition, both mating combinations showed no differences in *HAS* (*HAS-1*, *HAS-2*, *HAS-3*) and *Hyal* (*Hyal-1*, *Hyal-2*, *Hyal-3*) mRNA in decidua on Gd 13.5.

Surprisingly, *HAS-1* mRNA could not be detected in placenta. The expression levels of *HAS-2*, *HAS-3*, *Hyal-1*, *Hyal-2* and *Hyal-3* mRNA did not differ between normal and spontaneous abortion mouse models in placenta (Fig. 3). Although no changes were observed in

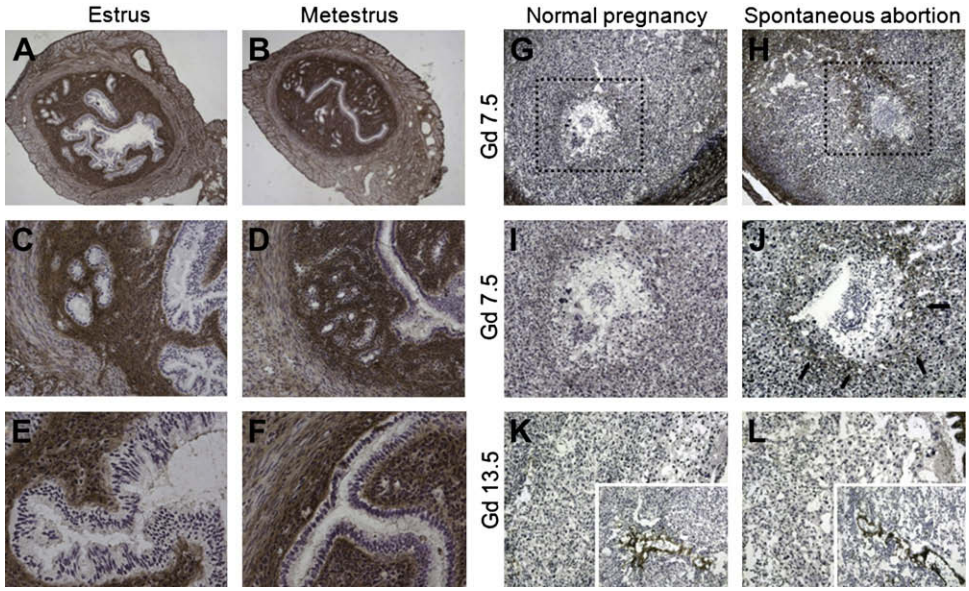

Fig. 2. Histochemical localization of HA. Representative examples of HA histochemistry in non-pregnant mouse uterus from estrus (A) and metestrus (B) period (Magnification: A–B × 50). Panels 2C (×100) and 2E (×200) correspond to magnification of 2A, while 2D (×100) and 2F (×200) correspond to 2B. HA expression was also evaluated in decidua (G–J) and placenta (K and L) from normal pregnancy and spontaneous abortion. Arrows depict HA presence around the embryo crypt in spontaneous abortion (J). In placenta, HA expression surrounding umbilical blood vessels is shown (K and L inserts). Magnification: G–H × 25 and I–J × 50.

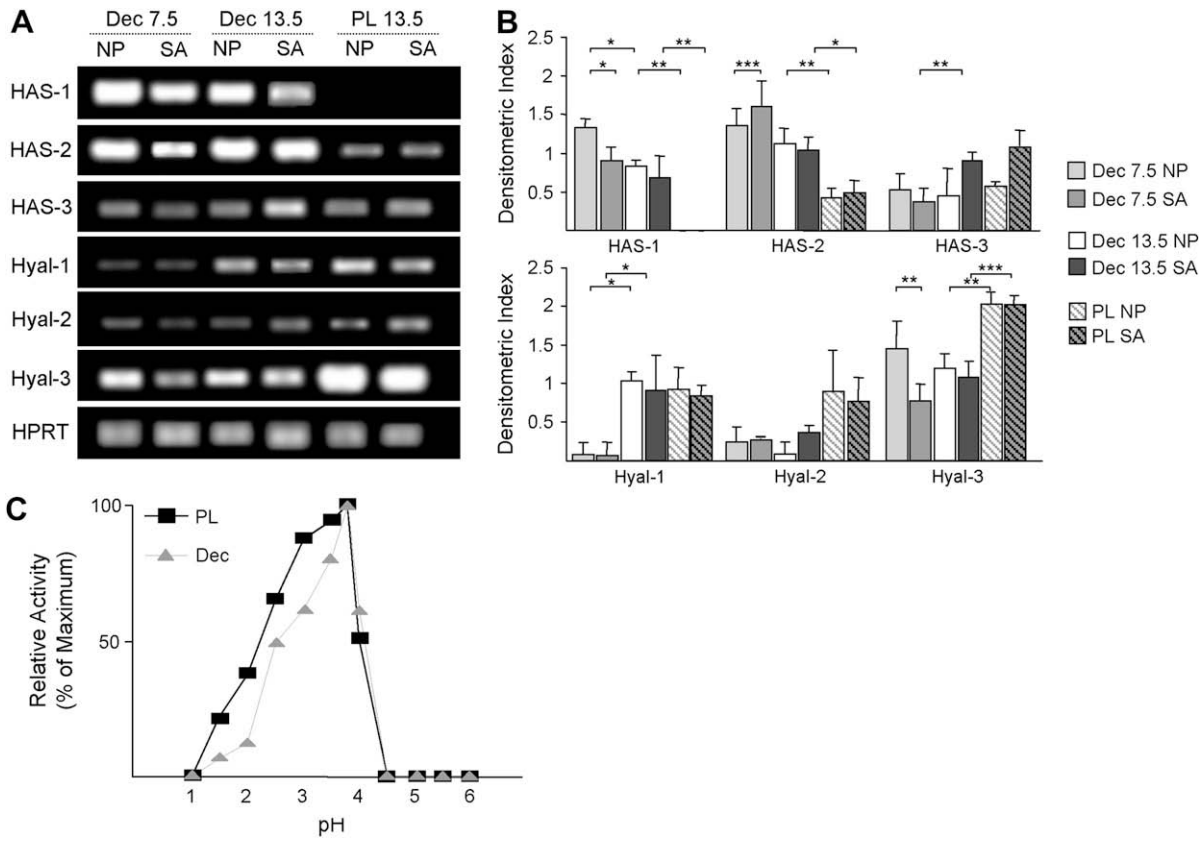

Fig. 3. HA synthesis and degradation. (A) HAS (*HAS-1*, *HAS-2* and *HAS-3*) and Hyal (*Hyal-1*, *Hyal-2* and *Hyal-3*) mRNA expression analyzed by *RT-PCR* in decidua (Dec) and placenta (PL) from normal pregnancy and spontaneous abortion. *Hprt* gene was used as control of near equal amplification. In decidua, the enzymes were evaluated on Gd 7.5 and 13.5, while in placenta on Gd 13.5. One representative from three independent experiments is shown. (B) Densitometric analysis of the bands observed in (A). The results are expressed as Index (*HAS* or *Hyal* mRNA expression/*hprt* mRNA expression), determined from three independent experiments and normalized to the reference gene. Bars represent mean ± SD; *indicate $p < 0.05$; **$p < 0.01$; ***$p < 0.001$. (C) pH activity profile of Hyal activity in decidua (Dec) and placenta (PL). The profiles were determined by incubating HA-coated wells with tissue extracts in Hyal assay buffer at various pH values (1.5–6.5). Control wells were only incubated with Hyal buffers of specified pH. Hyal activity at each pH was calculated as (Absorbance control − Absorbance sample) × 100. The maximum difference was designated as 100%, and the data is expressed as Relative Activity (percentage of maximum).

Hyal-3 mRNA expression between these two mating groups, it is noteworthy that placental *Hyal-3* mRNA levels were remarkably enhanced compared to decidual levels ($p < 0.01$).

To sum up, analysis of HAS and Hyal pattern of expression on Gd 7.5 showed that *HAS-1* and *HAS-2* mRNA were decreased in decidua from spontaneous abortion compared to normal pregnancy, while *Hyal-3* mRNA was increased in normal pregnancy. This difference in HAS/Hyal balance could be responsible for decidual HA increased levels observed in spontaneous abortion. In placenta, absence of *HAS-1* mRNA expression and increased levels of *Hyal-3* mRNA correlate with decreased levels of HA.

3.4. Characterization and detection of uterine and placental derived hyaluronidase activity

To confirm the functionality of the *Hyal* mRNAs detected, we tested hyaluronidase (Hyal) activity using an ELISA like assay. First, we assessed the pH activity profile of Hyals present at decidua and placenta from normal pregnancy mice by evaluating Hyal activity at different pH values. As shown in Fig. 3C, we found that Hyal activity presented a similar acidic pH profile with an optimum pH = 3.8 for HA degradation both in decidua and placenta. Interestingly, the Hyals were active at pH = 1.5 but not at pH = 4.5, this seems to be a hallmark of these tissues. Then, we analyzed Hyal activity in decidua and placenta obtained from non-pregnant, normal pregnancy and spontaneous abortion mice. Surprisingly, we found that Hyal activity in non-pregnant uteri, decidua and placenta were very similar. Indeed, levels were below 5 mU/mg and no significant differences were observed between normal pregnancy and spontaneous abortion ($p > 0.05$) (Table 2).

In summary, we were able to characterize the pH activity profile of Hyals from decidua and placenta. Besides, our results showed low Hyal activity in decidua and placenta, but it was not possible to detect differences between normal pregnancy and spontaneous abortion.

3.5. Analysis of HA molecular size

As HA polymers exist in a variety of sizes that have a large array of properties, we further analyzed the molecular size of the HA present in uteri and placenta from non-pregnant, normal pregnancy and spontaneous abortion mice. Structural studies on the HA

Table 2
Measurement of Hyal activity in uterine and placenta tissue extracts.

Tissue	Hyal activity (milliunits/mg)
Non-pregnant uterus	3.0 ± 1.5
Decidua NP Gd 7.5	4.0 ± 0.8
Decidua SA Gd 7.5	4.7 ± 1.5
Decidua NP Gd 13.5	2.7 ± 1.0
Decidua SA Gd 13.5	2.4 ± 0.5
Placenta NP Gd 13.5	2.2 ± 0.6
Placenta SA Gd 13.5	2.1 ± 0.6

NP: normal pregnancy; SA: spontaneous abortion; Gd: Gestation day.

molecular size were carried out using FPLC analysis, in order to separate intact mature HA molecule from its degradation fragments (oligosaccharides). The analysis of eluted peaks was performed by FACE of unsaturated disaccharides obtained after specific enzymatic treatment and AMAC derivatization.

Chromatographic data showed that non-pregnant uteri contain large HA molecules of about 2015 kDa included in a single peak (Fig. 4A). During normal pregnancy on Gd 7.5, FPLC analysis showed that HA presence was not identifiable with a single peak, but with the elution of material with a broad molecular size ranging from 1930 to 1530 kDa (Fig. 4B). However, when decidua from spontaneous abortion mice was evaluated, HA molecules of 2020 and 1620 kDa in two separate peaks were found (Fig. 4C). We also investigated HA molecular size in decidua on Gd 13.5 finding that both extracts derived from normal pregnancy and spontaneous abortion contain HA molecules of lower molecular size (about 1590 and 1620 kDa respectively) included in a single peak (Fig. 4D and E).

Furthermore, chromatographic data from placenta showed that both in normal pregnancy and spontaneous abortion HA molecules eluted only in one well-defined peak of similar molecular size (1660 and 1840 kDa respectively) (Fig. 4F and G). It is noteworthy that in these graphics the area under the peak does not represent HA concentration.

To sum up, differences in HA molecular size distribution were observed between normal pregnancy and spontaneous abortion on Gd 7.5. Indeed, in decidua from normal pregnancy HA molecules presented a broad molecular size ranging from 1930 to 1530 kDa, while in spontaneous abortion only HA molecules of 2020 and 1620 kDa were found.

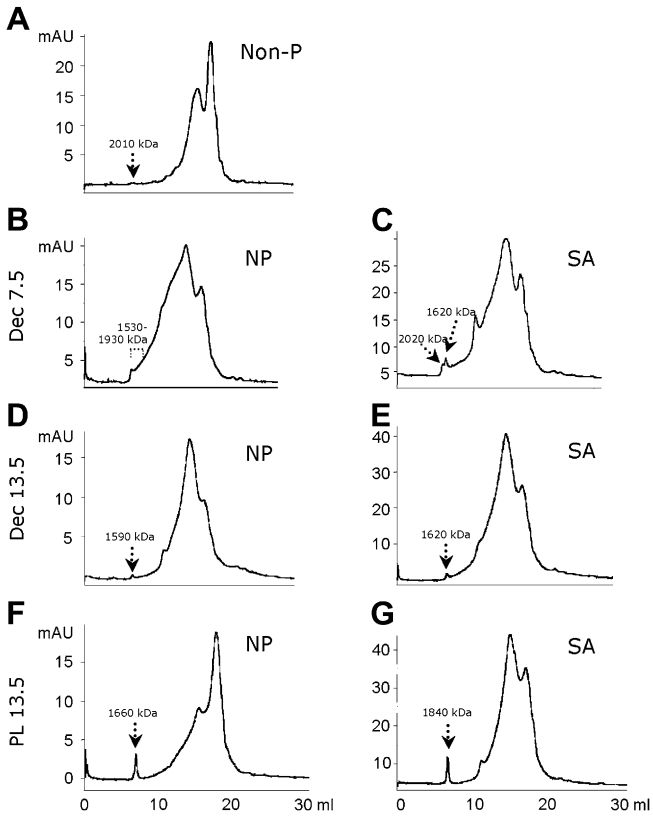

Fig. 4. Analysis of HA molecular size during pregnancy. Gel filtration chromatography of GAGs extracted from decidua (B–E) or placenta (F and G) of normal pregnancy and spontaneous abortion mice (left and right panels respectively). In Fig. 4 A, uterus from non-pregnant mice is depicted. The arrows indicate the calculated molecular mass of HA containing peaks. Non-P: non-pregnant; NP: normal pregnancy; SA: spontaneous abortion; Dec: decidua and PL: placenta.

4. Discussion

Establishment of pregnancy constitutes a unique situation in which the integrated action of delicate immunoregulatory mechanisms as well as endometrial modifications (including alterations in ECM components such as HA) occurs.

In the present work, we observed differential systemic and local HA levels and distribution during normal pregnancy and spontaneous abortion. Serum HA levels during pregnancy have been assessed by Uchiyama et al., observing that HA increases during pregnancy [29]. Accordingly, our results show that both serum and decidual HA levels increase during normal pregnancy. Nevertheless, such increase could not be detected in spontaneous abortion mice. Furthermore, HA levels in this group were clearly decreased in serum compared to decidua. These findings show a good correlation between systemic (serum) and local (decidual) HA levels in normal pregnancy but not in spontaneous abortion. This is particularly interesting because it indicates that noninvasive serum HA measurement is able to reflect decidual HA deposition during normal pregnancy in mice. On the other hand, lack of correlation between serum and decidual HA levels in spontaneous abortion denotes an alteration in HA turn over which would be responsible for HA accumulation in decidua. This is further supported by the increased decidual HA concentration found in spontaneous abortion on Gd 7.5.

Histochemical staining showed that on Gd 7.5 HA was localized in the myometrium as well as in mesometrial decidua but not in the antimesometrial one. Similar results were previously observed by Brown et al. and San Martin et al., who have proposed that adequate HA levels may facilitate implantation because of its ability to expand the extracellular space and allow blastocyst adhesion. Moreover, HA presence in the mesometrial region has been associated with cell proliferation and angiogenesis, which are processes connected with placental establishment. In addition, clearance of HA from the antimesometrial decidua has been postulated to be part of a maternal program to restrict trophoblast invasion during implantation [17,19]. Interestingly, HA positive staining was also found surrounding the embryo crypt in spontaneous abortion samples. The latter finding is in accordance with increased decidual HA levels observed in this mating combination. Since Gd 7.5 is the day before onset of rejection our results led us to hypothesize that although HA may be required for adequate implantation (on Gd 4), after this process elevated HA expression with inadequate localization would be involved in pregnancy failure. During morphogenesis, a decrease in HA would be necessary to induce adequate signals in proliferating and migrating cells. In fact, transition between high and low HA levels promotes initiation of cell interactions essential for differentiation, while elevated HA levels inhibit this process [6]. Therefore, we suggest that HA accumulation would result in abnormal ECM-cell signals leading to pregnancy failure.

Low HA levels were observed in placenta from both normal and pathological pregnancies. Besides, HA histochemistry revealed its absence in trophoblast cells with positive regions surrounding umbilical blood vessels. These results are in line with previous reports in human placenta in which HA was observed in the villous stroma but not in trophoblast cells during the first trimester. Moreover, HA staining was concentrated around central blood vessels and was associated with regulation of angiogenesis [18].

We also evaluated HA presence in different phases of the estrous cycle in non-pregnant mice. Both in estrus and metestrus, a strong HA positive signal in endometrial stroma could be detected with no HA expression in the lumen or glands. In humans, distribution of HA across the menstrual cycle has shown peaks of stromal deposition [30]. One peak has been observed before ovulation during the mid proliferative phase corresponding to the time of proliferation, while a second peak has been found after ovulation in the mid

secretory phase when the tissue is receptive to embryo implantation. Besides, during the mid secretory phase HA staining was strongly positive between the glands and around blood vessels. Although there are remarkable differences between mouse estrous and human menstrual cycles, it is interesting to note that in both kinds of cycle elevated HA levels were found in stages surrounding ovulation.

Since accumulation of HA is the outcome of a balance between the activity of HAS and Hyals, we investigated the relationship between HA and HAS/Hyal expression profiles in normal and pathological pregnancies [31]. On the one hand, RT-PCR demonstrated mRNA expression of *HAS-1*, *HAS-2* and *HAS-3* in decidua both of normal pregnancy and spontaneous abortion, but with a predominance of *HAS-1* and *HAS-2*. However, only *HAS-2* and *HAS-3* were expressed in placenta with no evidence of *HAS-1* mRNA. HAS isozymes present different enzymatic properties [32]. For example, HAS-1 and HAS-2 produce large forms of HA (200–2000 kDa) while HAS-3 produces smaller HA polymers (100–1000 kDa). As HA has a wide variety of roles which are size dependent, its functions could be regulated through control of the expression of HAS isozymes. On the other hand, mRNA expression of *Hyal-1*, *Hyal-2* and *Hyal-3* was observed both in decidua and placenta. It was interesting that *Hyal-3* was the most expressed Hyal, being even higher in placenta. *Hyal-1*, *Hyal-2* and *Hyal-3* mRNA have been previously detected in uterine and placental tissues [33]. Among the Hyal isoforms, HYAL-1 and HYAL-2 are the most studied ones and together with CD44 cell surface receptor are of great importance in degradation of HMW-HA [8,34]. HYAL-1 is an acid active lysosomal enzyme that cleaves HA to fragments of 4 disaccharide units, while HYAL-2 is an enzyme anchored to the plasma membrane that digests HMW-HA into fragments of 50 disaccharide units [35]. Although broadly expressed, HYAL-3 function is still unknown. Hyal-3 expression is up regulated by inflammatory cytokines in chondrocytes [36]. Besides, HYAL-3 has also been identified in bladder and prostate tumor cells. However, its activity has not been assessed *in vitro* up to date [36,37].

Comparison of HAS/Hyal expression patterns between normal pregnancy and spontaneous abortion on Gd 7.5 showed that HAS-1 as well as HAS-2 mRNA were decreased in decidua from spontaneous abortion, while Hyal-3 expression was increased in normal pregnancy. Since HA levels were elevated in decidua from spontaneous abortion, these findings led us to hypothesize that it is the modulation of Hyal-3 what provides rapid response mechanisms for changing HA levels. Moreover, reduced HA levels in placenta can be related to absence of HAS-1 and increased Hyal-3 mRNA. In addition, no differences in HAS/Hyal expression pattern on Gd 13.5 between normal and pathological pregnancies were in accordance with no changes in HA levels. Thus, we investigated Hyal activity finding that both decidual and placental Hyals presented an acidic pH profile with optimum activity at pH 3.8. These findings are in line with previous studies showing that human placental Hyals present optimal activity between pH 3.5 and 4.0 [38]. Furthermore, no differences in Hyal activity could be observed between normal and pathological pregnancies. Taken together: our results suggest that decidual and placental Hyal activity would be due to Hyal-1 and Hyal-2, since no significant differences in Hyal-1 and Hyal-2 mRNA expression or activity could be observed between normal and pathological pregnancies. We had suggested that elevated HA levels in spontaneous abortion were due to diminished Hyal-3 expression and accordingly would have expected an overall decrease in Hyal activity. We were nevertheless unable to detect Hyal-3 activity, probably due to the limitations of the actual techniques for measurement of Hyal activity. Hyal-3 function remains being a mystery but considering our results, it is clear that Hyal-3 must have an important role in HA clearance at the fetomaternal interface.

We also investigated HA size at the fetomaternal unit. Interestingly, only HMW-HA was found at any of the stages studied of both normal and pathological pregnancies. This was in agreement with observation of predominant HAS-1 and/or HAS-2 expression which produce large forms of HA. Further, our study denoted a difference in HA metabolism between normal pregnancy and spontaneous abortion mice. Indeed, on Gd 7.5 HA molecules of 2020 and 1620 kDa were found in decidua from spontaneous abortion, while in normal pregnancy HA molecules presented a broad molecular size ranging from 1930 to 1530 kDa indicating an active process of synthesis and degradation. Although in both cases we were in presence of HMW-HA, it is evident that HA metabolism in spontaneous abortion differs from normal pregnancy. Further research is nevertheless required to elucidate whether this difference in HA metabolism is associated with a differential balance in HAS/Hyal expression and/or with nonenzymatic fragmentation, and how it relates to pregnancy failure.

High rates of spontaneous abortion in the CBA/J $\times$ DBA/2J mating combination have provided a valuable model for defining mechanisms leading to pregnancy loss [39]. It has been shown that increased Th1 cytokine levels produced by macrophages, NK and T cells induce an inflammatory process with deleterious effects on pregnancy, while an anti-inflammatory response induced by Th2 cytokines appears to be pregnancy-protective [40]. Besides, presence of a mature DC phenotype correlates with higher abortion rates [41]. TLR-4 is also a known mediator of signals leading to spontaneous abortion in the CBA $\times$ DBA/2 model, and anti-TLR-4 reduces the rate of abortion [42]. It has been observed that HA fragments – but not HMW-HA - are able to induce phenotypic and functional DC maturation through TLR-4 [43]. However, low doses ($\sim$1 μg/ml) of HMW-HA are also able to activate DCs through a CD44-independent pathway, being TLR-4 one of the possible receptors involved [44]. In addition, biosynthesis of HA on endothelial cells can be regulated by proinflammatory stimuli (LPS, IL-1β, TNF-α, and IL-15) [11]. Our results showed accumulation of HMW-HA around the embryo crypt in spontaneous abortion, which would be able to generate alterations in ECM-cell interactions contributing to pregnancy failure. Whether HA accumulation is the cause or the consequence of proinflammatory signals leading to pregnancy failure, as well as the mechanisms by which HA would contribute to abortion remain to be elucidated.

In summary, in the present work we showed increased decidual HA levels in spontaneous abortion compared with normal pregnancy mice on Gd 7.5. In addition, this is the first time HA molecular size has been characterized at the fetomaternal interface, finding HMW-HA both in normal and pathologic pregnancies. Moreover, HA metabolism seems to be altered in spontaneous abortion as shown by a decrease in Hyal-3 expression as well as by differences in the molecular size spectrum of HA. This alteration in HA metabolism could explain HA increase and its abnormal distribution around the embryo implantation crypt. We believe that along with other mechanisms, increased HA levels in decidua would contribute to pregnancy failure. Our work constitutes a great contribution to HA field where correlation between *in vitro* and *in vivo* findings is required. However, further studies are necessary to completely clarify HA metabolism during spontaneous abortion and to understand the role of HA in the pathogenesis of murine as well as human pregnancy failure.

Acknowledgments

We are indebted with Dr. P.C. Arck for comments on the manuscript. We are grateful to Farmatrade Argentina for providing HMW-HA. R.C-R. and G.B. thank the German Academic Exchange Program (DAAD) for the fellowships granted. M.G.G is a guest scientist at the Charité, supported by the Alexander von Humboldt

Foundation in Germany. S.M.B is a fellow of the Habilitation program at Charité, University Medicine Berlin. A.O. is supported by the Turkish Higher Education Council. M.G.G., L.A. and S.H are members of the Scientific Career of CONICET. This work was supported by research grant from Charité to S.M.B.

References

[1] Duc-Goiran P, Mignot TM, Bourgeois C, Ferre F. Embryo-maternal interactions at the implantation site: a delicate equilibrium. Eur J Obstet Gynecol Reprod Biol 1999;83(1):85–100.
[2] Wang H, Dey SK. Roadmap to embryo implantation: clues from mouse models. Nat Rev Genet 2006;7(3):185–99.
[3] Malassiné A, Frendo JL, Evain-Brion D. A comparison of placental development and endocrine functions between the human and mouse model. Hum Reprod Update 2003;9(6):531–9.
[4] Sharkey AM, Smith SK. The endometrium as a cause of implantation failure. Best Pract Res Clin Obstet Gynaecol 2003;17(2):289–307.
[5] Stamenkovic I. Extracellular matrix remodelling: the role of matrix metalloproteinases. J Pathol 2003;200(4):448–64.
[6] Toole BP. Hyaluronan in morphogenesis. Semin Cell Dev Biol 2001;12(2):79–87.
[7] Weigel PH, DeAngelis PL. Hyaluronan synthases: a decade-plus of novel glycosyltransferases. J Biol Chem 2007;282(51):36777–81.
[8] Csoka AB, Frost GI, Stern R. The six hyaluronidase-like genes in the human and mouse genomes. Matrix Biol 2001;20(8):499–508.
[9] Paiva P, Van Damme MP, Tellbach M, Jones RL, Jobling T, Salamonsen LA. Expression patterns of hyaluronan, hyaluronan synthases and hyaluronidases indicate a role for hyaluronan in the progression of endometrial cancer. Gynecol Oncol 2005;98(2):193–202.
[10] Jiang D, Liang J, Noble PW. Hyaluronan in tissue injery and repair. Annu Rev Cell Dev Biol 2007;23:435–61.
[11] Mummert ME. Immunologic roles of hyaluronan. Immunol Res 2005;31(3):189–206.
[12] Toole BP. Hyaluronan: from extracellular glue to pericellular cue. Nat Rev Cancer 2004;4(7):528–39.
[13] Turley EA, Noble PW, Bourguignon LY. Signaling properties of hyaluronan receptors. J Biol Chem 2002;277(7):4589–92.
[14] Deed R, Rooney P, Kumar P, Norton JD, Smith J, Freemont AJ, et al. Early-response gene signalling is induced by angiogenic oligosaccharides of hyaluronan in endothelial cells. Inhibition by non-angiogenic, high-molecular-weight hyaluronan. Int J Cancer 1997;71(2):251–6.
[15] Termeer CC, Hennies J, Voith U, Ahrens T, Weiss JM, Prehm P, et al. Oligosaccharides of hyaluronan are potent activators of dendritic cells. J Immunol 2000;165(4):1863–70.
[16] Carson DD, Dutt A, Tang JP. Glycoconjugate synthesis during early pregnancy: hyaluronate synthesis and function. Dev Biol 1987;120(1):228–35.
[17] Brown JJ, Papaioannou VE. Distribution of hyaluronan in the mouse endometrium during the periimplantation period of pregnancy. Differentiation 1992;52(1):61–8.
[18] Goshen R, Ariel I, Shuster S, Hochberg A, Vlodavsky I, de Groot N, et al. Hyaluronan, CD44 and its variant exons in human trophoblast invasion and placental angiogenesis. Mol Hum Reprod 1996;2(9):685–91.
[19] San Martin S, Soto-Suazo M, Zorn TM. Distribution of versican and hyaluronan in the mouse uterus during decidualization. Braz J Med Biol Res 2003;36(8):1067–71.
[20] Blois S, Zenclussen AC, Roux ME, Olmos S, di Conza J, Arck PC, et al. Asymmetric antibodies (Aab) in the female reproductive tract. J Reprod Immunol 2004;64(1–2):31–43.
[21] Garcia MG, Tirado-Gonzalez I, Handjiski B, Tometten M, Orsal AS, Hajos SE, et al. High expression of survivin and down-regulation of Stat-3 characterize the feto-maternal interface in failing murine pregnancies during the implantation period. Placenta 2007;28(7):650–7.
[22] Sugahara KN, Hirata T, Hayasaka H, Stern R, Murai T, Miyasaka M. Tumor cells enhance their own CD44 cleavage and motility by generating hyaluronan fragments. J Biol Chem 2006;281(9):5861–8.
[23] Jameson JM, Cauvi G, Sharp LL, Witherden DA, Havran WL. Gammadelta T cell-induced hyaluronan production by epithelial cells regulates inflammation. J Exp Med 2005;201(8):1269–79.
[24] Mummert ME, Mummert D, Edelbaum D, Hui F, Matsue H, Takashima A. Synthesis and surface expression of hyaluronan by dendritic cells and its potential role in antigen presentation. J Immunol 2002;169(8):4322–31.
[25] Stern M, Stern R. An ELISA-like assay for hyaluronidase and hyaluronidase inhibitors. Matrix 1992;12(5):397–403.
[26] Raio L, Cromi A, Ghezzi F, Passi A, Karousou E, Viola M, et al. Hyaluronan content of Wharton's jelly in healthy and down syndrome fetuses. Matrix Biol 2005;24(2):166–74.
[27] Calabro A, Benavides M, Tammi M, Hascall VC, Midura RJ. Microanalysis of enzyme digests of hyaluronan and chondroitin/dermatan sulfate by fluorophore-assisted carbohydrate electrophoresis (FACE). Glycobiology 2000;10(3):273–81.
[28] Karousou EG, Militsopoulou M, Porta G, De Luca G, Hascall VC, Passi A. Polyacrylamide gel electrophoresis of fluorophore-labeled hyaluronan and chondroitin sulfate disaccharides: application to the analysis in cells and tissues. Electrophoresis 2004;25(17):2919–25.
[29] Uchiyama T, Sakuta T, Kanayama T. Regulation of hyaluronan synthases in mouse uterine cervix. Biochem Biophys Res Commun 2005;327(3):927–32.
[30] Salamonsen LA, Shuster S, Stern R. Distribution of hyaluronan in human endometrium across the menstrual cycle. Implications for implantation and menstruation. Cell Tissue Res 2001;306(2):335–40.
[31] Adamia S, Maxwell CA, Pilarski LM. Hyaluronan and hyaluronan synthases: potential therapeutic targets in cancer. Curr Drug Targets Cardiovasc Haematol Disord 2005;5:3–14.
[32] Itano N, Sawai T, Yoshida M, Lenas P, Yamada Y, Imagawa M, et al. Three isoforms of mammalian hyaluronan synthases have distinct enzymatic properties. J Biol Chem 1999;274(35):25085–92.
[33] Patel S, Turner PR, Stubberfield C, Barry E, Rohlff CR, Stamps A, et al. Hyaluronidase gene profiling and role of hyal-1 overexpression in an orthotopic model of prostate cancer. Int J Cancer 2002;97(4):416–24.
[34] Harada H, Takahashi M. CD44-dependent intracellular and extracellular catabolism of hyaluronic acid by hyaluronidase-1 and -2. J Biol Chem 2007;282(8):5597–607.
[35] Stern R. Hyaluronan metabolism: a major paradox in cancer biology. Pathol Biol 2005;53(7):372–82.
[36] Flannery CR, Little CB, Hughes CE, Caterson B. Expression and activity of articular cartilage hyaluronidases. Biochem Biophys Res Commun 1998;251(3):824–9.
[37] Lokeshvar VB, Schroeder GL, Carey RI, Soloway MS, Iida N. Regulation of hyaluronidase activity by alternative mRNA splicing. J Biol Chem 2002;277(37):33654–63.
[38] Fiszer-Szafarz B, Litynska A, Zou L. Human hyaluronidases: electrophoretic multiple forms in somatic tissues and body fluids. Evidence for conserved hyaluronidase potential N-glycosylation sites in different mammalian species. J Biochem Biophys Methods 2000;45(2):103–16.
[39] Clark DA, Coulam CB, Daya S, Chaouat G. Unexplained sporadic and recurrent miscarriage in the new millennium: a critical analysis of immune mechanisms and treatments. Hum Reprod Update 2001;7(5):501–11.
[40] Blois SM, Joachim R, Kandil J, Margni R, Tometten M, Klapp BF, et al. Depletion of $CD8^+$ cells abolishes the pregnancy protective effect of progesterone substitution with dydrogesterone in mice by altering the Th1/Th2 cytokine profile. J Immunol 2004;172(10):5893–9.
[41] Blois SM, Kammerer U, Alba Soto C, Tometten MC, Shaikly V, Barrientos G, et al. Dendritic cells: key to fetal tolerance? Biol Reprod 2007;77(4):590–8.
[42] Kim YM, Romero R, Oh SY, Kim CJ, Kilburn BA, Armant R, et al. Toll-like receptor 4. A potential link between "danger signals", the innate immune system, and preeclampsia? Am J Obstet Gynecol 2005;193:921.e1–8.
[43] Termeer C, Benedix F, Sleeman J, Fieber C, Voith U, Ahrens T, et al. Oligosaccharides of hyaluronan activate dendritic cells via toll-like receptor 4. J Exp Med 2002;195(1):99–111.
[44] Do Y, Nagarkatti PS, Nagarkatti M. Role of CD44 and hyaluronic acid (HA) in activation of alloreactive and antigen-specific T cells by bone marrow-derived dendritic cells. J Immunother 2004;27(1):1–12.